  Bull. Chem. Soc. Jpn., 56, 2355—2362 (1983)

Reactions of NH Radicals. II. Photolysis of HN_3 in the Presence of C_2H_6 at 313 nm

Sukeya KODAMA

Department of Applied Chemistry, College of Engineering, University of Osaka Prefecture, Sakai, Osaka 591

(Received September 13, 1982)

Photolysis of HN_3 vapor with C_2H_6 was studied at 313 nm and 30 °C. The products are N_2, H_2, CH_4, NH_4N_3, $CH_3NH_2 \cdot HN_3$, $C_2H_5NH_2 \cdot HN_3$, CH_3N_3, and CH_3CN. The quantum yields of these products were measured as a function of pressures of HN_3 and C_2H_6, and the light intensity. The following mechanism for the main reactions was proposed: $HN_3+h\nu(313\text{ nm}) \rightarrow N_2+NH(a^1\Delta)$; $NH(a^1\Delta)+HN_3 \rightarrow 2N_2+2H$ (2a); $NH(a^1\Delta)+HN_3 \rightarrow NH_2+N_3$ (2b); $NH(a^1\Delta)+HN_3 \rightarrow N_2+N_2H_2^*$ (2c); $NH(a^1\Delta)+C_2H_6 \rightarrow C_2H_5NH_2^*$ (3); $NH(a^1\Delta)+C_2H_6 \rightarrow NH(X^3\Sigma^-)+C_2H_6$ (4); $C_2H_5NH_2^* \rightarrow CH_3+CH_2NH_2$ (5); $C_2H_5NH_2^* \rightarrow CH_3CN+2H_2$ (6); $C_2H_5NH_2^*+M \rightarrow C_2H_5NH_2+M$ (7). The rate constant ratios at 30 °C are: $k_3/k_2=0.334$; $k_4/k_2=0.217$; $k_6/k_5=0.038$. The values of k_7/k_5 for C_2H_6, HN_3, CO_2, and Xe are 36.5, 30.3, 29.0, and 14.5 $dm^3\ mol^{-1}$, respectively. The values of $k_5=9.8\times10^9\ s^{-1}$, $k_6=3.7\times10^8\ s^{-1}$, τ (half life of $C_2H_5NH_2^*$)$=6.8\times10^{-11}$ s, η (collisional deactivation efficiency of $C_2H_5NH_2^*$)$=1$ for C_2H_6, HN_3, and CO_2, and $\eta=0.60$ for Xe were obtained by using the collision theory.

In the previous work,[1] on the photolysis of HN_3 vapor at 313 nm, it was found that hydrazoic acid is a good radical source for the first excited singlet $NH(a^1\Delta)$. Therefore, the formation of amines by insertion of the singlet NH into the C–H bond is expected in the photolysis of HN_3 with hydrocarbons, because the insertion is a characteristic reaction of the excited singlet species as were found in the reactions of $O(^1D)$,[2] $S(^1D)$,[3] and $CH_2(^1A_1)$[4] with hydrocarbons.

Miller[5] has demonstrated the formation of amines in the photolysis of HN_3 with propane, butane, isobutane, and neopentane. Cornell *et al.*[6] have studied the flash and steady photolyses of HN_3 (DN_3) with hydrocarbons including methane and ethane. They have found that the principal nitrogen-containing products are HCN and alkanenitriles in the steady photolysis. Brash and Back[7] have investigated the photolysis of HNCO in the presence of ethane, propane, neopentane, *etc.* but no amines could be detected. Recently, Tsunashima *et al.*[8] have studied the photolysis of HN_3 in liquid ethane, propane, and isobutane at the Dry Ice–methanol temperature, and observed the formation of ethylamine from ethane, propyl- and isopropylamine from propane, and isobutyl- and *t*-butylamine from isobutane.

In the work, C_2H_6 was chosen as a reactant by the following reasons: (a) the formation of ethylamine by collisional stabilization of chemically excited $C_2H_5NH_2^*$ produced by the insertion may be expected in the vapor phase photolysis, although CH_3NH_2 could not be detected in the case of CH_4,[5] because $C_2H_5NH_2$ has more degrees of internal freedom than CH_3NH_2; and (b) the identification and the quantitative analysis of amines are easy, because C_2H_6 has only primary hydrogen as compared with higher hydrocarbons that have secondary and tertiary hydrogens. Thus, the photolysis of HN_3 with C_2H_6 in the gas phase at 313 nm and 30 °C has been carried out in the present work to obtain quantitative results.

Experimental

Reaction Procedure. Ethane obtained from Takachiho Chemical Co. was 99.8% pure. It was purified each time before use by condensation and evacuation at −160 °C and liquid nitrogen temperature. Preparation and purification of HN_3, and the reaction apparatus were the same as described previously.[1] All runs in this work were carried out at 313 nm and 30 °C. The light intensity was controlled by screens, and the irradiation time was 20 to 390 min. The degree of conversion of HN_3 was only a few per cent for all runs. The reaction products were N_2, H_2, CH_4, NH_4N_3, $CH_3NH_2 \cdot HN_3$, $C_2H_5NH_2 \cdot HN_3$, CH_3N_3, and CH_3CN. On the other side, the formation of HCN was found in addition to above products at high light intensities.

Identifications of $CH_3NH_2 \cdot HN_3$ and $C_2H_5NH_2 \cdot HN_3$. An NMR spectrum of a D_2O solution of the white volatile products, condensed at the Dry Ice–acetone temperature, was

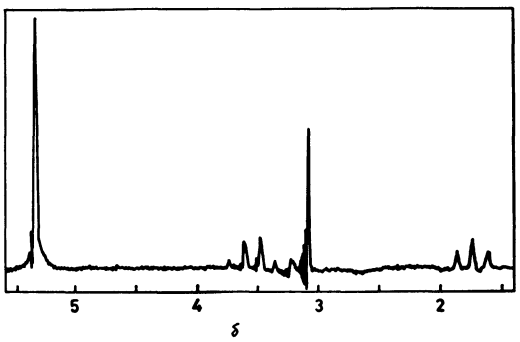

Fig. 1. NMR spectrum of a D_2O solution of the white volatile products trapped at the Dry Ice–acetone temperature.

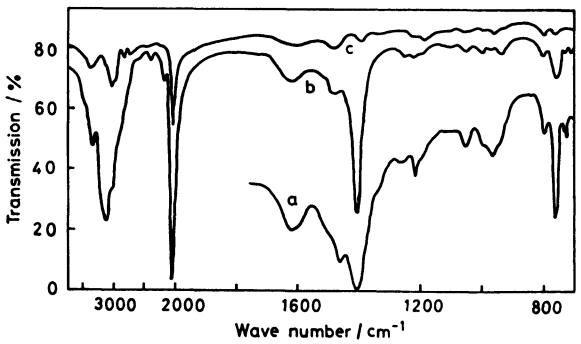

Fig. 2. IR spectra of the white volatile products (a and b) and $C_2H_5NH_2 \cdot HN_3$ sample (c).

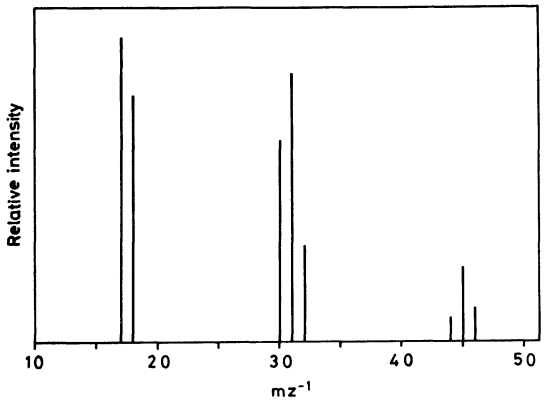

Fig. 3. Mass spectrum of the substances removed HN_3 from the white volatile products. The ionizing voltage is 15 eV.

obtained with a JNM 3H-60 (Japan Electron Optics) spectrometer, and is shown in Fig. 1. Chemical shifts are given in parts per million from $(CH_3)_4Si$. NMR spectra of known samples[9] of $CH_3NH_2 \cdot HN_3$, $C_2H_5NH_2 \cdot HN_3$, and $(CH_3)_2NH \cdot HN_3$ were also observed under the same conditions as above. From comparisons of the spectrum in Fig. 1 with the spectra of known samples, it was found that three peaks at 1.61, 1.73, and 1.85, a peak at 3.08, four peaks at 3.36, 3.48, 3.60, and 3.72, and a peak at 5.32 ppm correspond to the CH_3 group of ethylamine, CH_3 group of methylamine, CH_2 group of ethylamine, and NH_2 group of methyl- and ethylamine, respectively. Since a small peak at 3.20 ppm in Fig. 1 is in agreement with a peak of CH_3 group of $(CH_3)_2NH \cdot HN_3$ sample, the insertion of NH ($a^1\Delta$) into the C–C bond may be possible.

Infrared spectra of the white volatile products by the KBr disk method are shown in Fig. 2 together with a spectrum of a sample of $C_2H_5NH_2 \cdot HN_3$.[9] The main three peaks (1404, 2040, and 3150 cm^{-1}) in the spectra of the products are due to NH_4N_3,[1] and all peaks in the spectrum of the $C_2H_5NH_2 \cdot HN_3$ sample are found in the spectra of products as peaks or shoulders. The formation of $CH_3NH_2 \cdot HN_3$ could not be verified from the infrared spectra, because the spectrum of $CH_3NH_2 \cdot HN_3$ overlaps with the spectrum of $C_2H_5NH_2 \cdot HN_3$.

The white volatile products were introduced into a column of solid sodium hydroxide, then HN_3 molecules in the products ($RNH_2 \cdot HN_3$) were removed by the reaction,[8] $RNH_2 \cdot HN_3 + NaOH \longrightarrow RNH_2 + NaN_3 + H_2O$. A mass spectrum of the HN_3-removed products at the ionizing voltage of 15 eV is shown in Fig. 3. The existence of CH_3NH_2 and $C_2H_5NH_2$ together with NH_3 were verified from the masses of 17 (NH_3^+), 18 (NH_4^+), 30 (CH_3NH^+ or $CH_2NH_2^+$), 31 ($CH_3NH_2^+$), 32 ($CH_3NH_3^+$), 44 ($C_2H_5NH^+$ or $C_2H_4NH_2^+$), 45 ($C_2H_5NH_2^+$), and 46 ($C_2H_5NH_3^+$).

Quantitative Analysis of the Products. Noncondensable gases (N_2, H_2, and CH_4) at −210 °C were introduced into a column of silica gel (for gas chromatography) at −196 °C. Hydrogen, not trapped in the column, was collected in a Toepler gauge, and its amount determined. Nitrogen and methane, trapped on silica gel at −196 °C, were collected in the gauge by warming the column, and the total amount was also determined. The separation of N_2 and CH_4 was carried out by gas chromatography using a 5A molecular sieve column.

In the quantitative determinations of NH_4N_3, $CH_3NH_2 \cdot HN_3$, and $C_2H_5NH_2 \cdot HN_3$, the white volatile products condensed at the Dry Ice–acetone temperature were introduced on to a CuO column at about 550 °C. The combustion products were N_2, NO, CO_2, N_2O, and H_2O. The amounts of N_2 passing through a trap at −210 °C, NO trapped at −210 °C, and CO_2 and N_2O condensed at −196 °C were in turn determined by the Toepler gauge. H_2O was eliminated by trapping at −110 °C. The separation of CO_2 and N_2O was performed using a soda-lime column. The amount of CO_2 was determined by substracting the amount of N_2O from the total amount of CO_2 and N_2O.

From the stoichiometry for the combustion reactions, the relation, $[CO_2] = [CH_3NH_2 \cdot HN_3] + 2[C_2H_5NH_2 \cdot HN_3]$, is obtained for the CO_2 formation. On the other hand, the amount of $CH_3NH_2 \cdot HN_3$ can be estimated from the relation, $[CH_3NH_2 \cdot HN_3] = 0.540\,[CH_4]$, for all runs at low light intensities as discussed later. Therefore, the amount of $C_2H_5NH_2 \cdot HN_3$ can be calculated from the relation, $[C_2H_5NH_2 \cdot HN_3] = ([CO_2] - 0.540[CH_4])/2$. From the material balance of the nitrogen atoms, the amount of NH_4N_3 can be estimated by the equation, $[NH_4N_3] = (2[N_2] + 2[N_2O] + [NO])/4 - ([CO_2] + 0.540 \times [CH_4])/2$.

The quantum yields of products were measured by using HN_3 as an actinometer.[1]

Results

The results for the photolysis of HN_3 of 6.7 kPa, measured as a function of the absorbed light intensity at 313 nm, 30 °C, and 26.7 kPa of C_2H_6, are shown in Fig. 4. It is found in Fig. 4 that ϕ_{N_2}, ϕ_{CH_4}, $\phi_{CH_3NH_2 \cdot NH_3}$, and $\phi_{(CO_2)}(\phi_{CH_3NH_2 \cdot HN_3} + 2\phi_{C_2H_5NH_2 \cdot HN_3})$ decrease with an increase of the light intensity. The decrease of quantum yields seems due to radical-radical reactions, and the quantum yields converge to constant values at low light intensities. $\phi_{NH_4N_3}$, ϕ_{H_2}, and $\phi_{C_2H_5NH_2 \cdot HN_3}$ are independent of the light intensity.

Figure 5 shows the results of the photolysis measured as a function of C_2H_6 pressure at 6.7 kPa of HN_3 and low absorbed light intensity of 4.6×10^{14} quanta s^{-1} to eliminate radical-radical reactions. It is seen in Fig. 5 that ϕ_{N_2}, $\phi_{NH_4N_3}$, and ϕ_{H_2} decrease, and $\phi_{C_2H_5NH_2 \cdot HN_3}$ and $\phi_{(CO_2)}$ increase with an increase of C_2H_6 pressure, but ϕ_{CH_4} and $\phi_{CH_3NH_2 \cdot HN_3}$ decrease *via* each maximum value

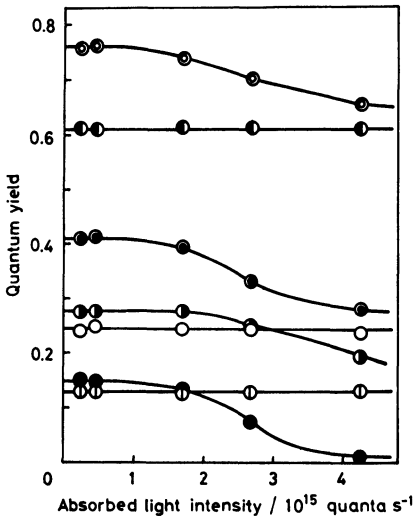

Fig. 4. Results for the photolysis of HN_3 of 6.7 kPa, measured as a function of the absorbed light intensity at 313 nm, 26.7 kPa of C_2H_6, and 30 °C. ◎, $\phi_{N_2}/5$; ◐, $\phi_{NH_4N_3}$; ⊙, $\phi_{(CO_2)}$; ◑, ϕ_{CH_4}; ○, ϕ_{H_2}; ⓘ, $\phi_{C_2H_5NH_2 \cdot HN_3}$; ●, $\phi_{CH_3NH_2 \cdot HN_3}$.

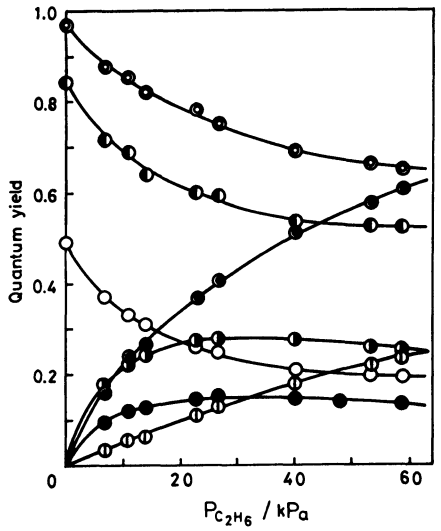

Fig. 5. Results of the photolysis of HN_3 of 6.7 kPa, measured as a function of C_2H_6 pressure at 313 nm, 30 °C, and low absorbed light intensity of 4.6×10^{14} quanta s^{-1}. The marks are the same as those in Fig. 4.

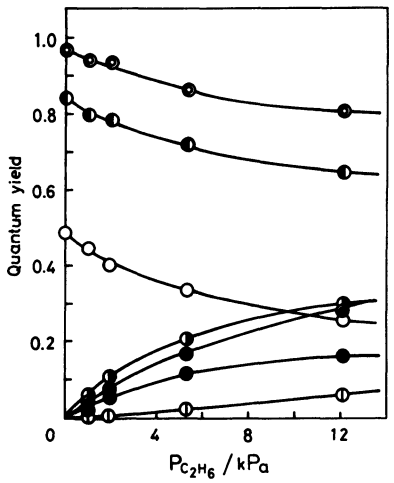

Fig. 6. Pressure dependence of C_2H_6 on the photolysis of HN_3 of 4.1 kPa at 313 nm, 30 °C, and low absorbed light intensity of 2.4×10^{14} quanta s^{-1}. The marks are the same as those in Fig. 4.

at about 27 kPa of C_2H_6.

The results for the photolysis of HN_3 at 4.1 kPa, measured as a function of C_2H_6 pressure, at low absorbed light intensity of 2.4×10^{14} quanta s^{-1} are shown in Fig. 6. In comparison with Fig. 5, it is seen from Fig. 6 that ϕ_{N_2} and ϕ_{H_2} decrease more rapidly, and ϕ_{CH_4} $\phi_{(CO_2)}$, and $\phi_{CH_3NH_2\cdot HN_3}$ increase more quickly as the C_2H_6 pressure increases.

Figure 7 shows the results of the photolysis, measured as a function of C_2H_6 pressure, at 6.7 kPa of HN_3 and high absorbed light intensity of 4.2×10^{15} quanta s^{-1}. It is seen in Fig. 7 that $\phi_{NH_4N_3}$ and ϕ_{H_2} are almost the same, but ϕ_{N_2}, $\phi_{(CO_2)}$, and ϕ_{CH_4} are lower as compared with those in Fig. 5.

Discussion

Reaction Mechanism. On the basis of the experimental results obtained above, the following reaction mechanism is postulated for the photolysis of HN_3 in the presence of C_2H_6 at low light intensities, where A, E, and M denote HN_3, C_2H_6, and deactivator molecules, respectively:

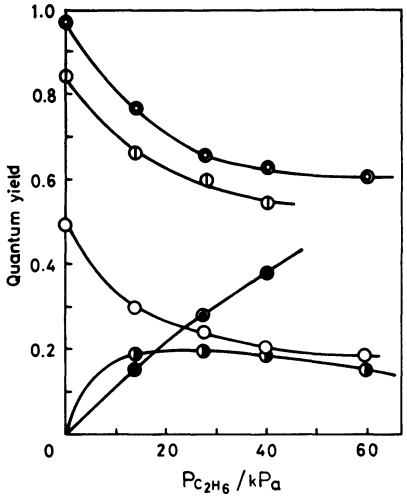

Fig. 7. Results of the photolysis of HN_3 of 6.7 kPa, measured as a function of C_2H_6 pressure at 313 nm, 30 °C, and high absorbed light intensity of 4.2×10^{15} quanta s^{-1}. The marks are the same as those in Fig. 4.

$$A + h\nu(313\text{ nm}) \longrightarrow N_2 + NH(a^1\Delta) \quad (1)$$

$$NH(a^1\Delta) + A \longrightarrow 2N_2 + 2H \quad (2a)$$

$$NH(a^1\Delta) + A \longrightarrow NH_2 + N_3 \quad (2b)$$

$$NH(a^1\Delta) + A \longrightarrow N_2 + N_2H_2^* \quad (2c)$$

$$NH(a^1\Delta) + E \longrightarrow C_2H_5NH_2^* \quad (3)$$

$$NH(a^1\Delta) + E \longrightarrow NH(X^3\Sigma^-) + E \quad (4)$$

$$C_2H_5NH_2^* \longrightarrow CH_3 + CH_2NH_2 \quad (5)$$

$$C_2H_5NH_2^* \longrightarrow 2H_2 + CH_3CN \quad (6)$$

$$C_2H_5NH_2^* + M \longrightarrow C_2H_5NH_2 + M \quad (7)$$

$$CH_2NH_2 + A \longrightarrow CH_3NH_2 + N_3 \quad (8)$$

$$CH_2NH_2 + A \longrightarrow CH_3N_3 + NH_2 \quad (9)$$

$$NH(X^3\Sigma^-) + A \longrightarrow H_2 + 2N_2 \quad (10)$$

$$NH(X^3\Sigma^-) + A \longrightarrow NH_2 + N_3 \quad (11)$$

$$H + A \longrightarrow H_2 + N_3 \quad (12)$$

$$H + A \longrightarrow NH_2 + N_2 \quad (13)$$

$$N_2H_2^* \longrightarrow N_2H_2^{**} \quad (14)$$

$$N_2H_2^* + A \longrightarrow N_2 + H_2 + A \quad (15)$$

$$N_2H_2^* + A \longrightarrow NH_3 + 2N_2 \quad (16)$$

$$N_2H_2^{**} + A \longrightarrow NH_3 + 2N_2 \quad (17)$$

$$CH_3 + A \longrightarrow CH_4 + N_3 \quad (18)$$

$$NH_2 + A \longrightarrow NH_3 + N_3 \quad (19)$$

$$N_3 + A \longrightarrow A\cdot N_3 \quad (20)$$

$$2A\cdot N_3 \longrightarrow 3N_2 + 2A \quad (21)$$

$$RNH_2(R=H,\ CH_3,\text{ and } C_2H_5) + A \longrightarrow RNH_2\cdot HN_3. \quad (22)$$

Thermochemical considerations were taken into account using the standard heats of formation listed in Table 1.

TABLE 1. SELECTED HEATS OF FORMATION*

	$\Delta H^{\circ}_{f'298}$ / kJ mol^{-1}	Ref.		$\Delta H^{\circ}_{f'298}$ / kJ mol^{-1}	Ref.
HN_3	299.8	a	C_2H_6	−84.7	e
$NH(a^1\Delta)$	506.6	b,c	CH_2CN	230.1	l
CH_3	146.9	d	CH_3CN	79.9	n
CH_4	−74.8	e	CH_3NC	150.2	o
CN	418.4	f	CH_2=C=NH	238.1	p
HCN	130.5	e	CH≡C–NH_2	222.2	p
CH_2=NH	94.6	g	CH_2CH_2N	297.5	q
CH_2NH_2	154.8	h	$C_2H_3NH_2$	48.5	p
CH_3NH	174.5	i	CH_3CH=NH	63.2	p
CH_3NH_2	−28.0	j	CH_3–N=CH_2	72.4	n
CH_3N_3	280.3	k	CH_2CH_2NH	104.6	r
C_2H_2	226.7	e	CH_3–N–CH_3	156.5	i
C_2H_3	267.8	l	CH_3CH_2NH	174	s
C_2H_4	52.3	e	$C_2H_5NH_2$	−48.5	j
C_2H_5	110.0	m	$(CH_3)_2NH$	−18.8	t

* See Table 1 in Ref. 1 for the heats of formation of NH ($X^3\Sigma^-$), N_3, NH_2, H, N_2H_2, NH_3, and NH_4N_3. a) P. Gray and T. C. Waddigton, *Proc. R. Soc. London, Ser. A*, **235**, 106 (1956). b) H. Okabe and M. Lenzi, *J. Chem. Phys.*, **47**, 5241 (1967). c) L. G. Piper, *J. Chem. Phys.*, **70**, 3417 (1979). d) M. H. Baghal-Vayjooee, A. J. Colussi, and S. W. Benson, *Int. J. Chem. Kinet.*, **11**, 147 (1979). e) "Handbook of Chemistry and Physics," 55th ed, ed by R. C. Weast, Chemical Ruffer Co. Press, Cleveland, OH (1974—1975). f) J. L. Franklin, J. G. Dillard, H. M. Rosenstock, J. T. Herron, K. Druxl, and F. H. Field, "Ionization Potentials, Appearance Potentials, and Heats of Formation of Gaseous Positive Ions," NSRDS-NBS 26, U. S. Government Printing Office, Washington D. C. (1969). g) A. J. Paine and J. Warkentin, *Can. J. Chem.*, **59**, 491 (1981). h) D. K. S. Sharma and J. L. Franklin, *J. Am. Chem. Soc.*, **95**, 6562 (1973). i) S. W. Benson and H. E. O'Neal, "Kinetic Data on Gas Phase Unimolecular Reactions," NSRDS-NBS-21, National Bureau of Standards Reference Data System, U. S. Department of Commerce, (1970). j) S. W. Benson and J. H. Buss, *J. Chem. Phys.*, **29**, 546 (1958). k) D. M. Golden, R. Walsh, and S. W. Benson, *J. Am. Chem. Soc.*, **87**, 4053 (1965). l) J. A. Kerr, *Chem. Rev.*, **66**, 465 (1966). m) M. Luria and S. W. Benson, *J. Am. Chem. Soc.*, **97**, 3342 (1975). n) S. W. Benson, F. R. Cruickshank, D. M. Golden, G. R. Haugen, H. E. O'Neal, A. S. Rodgers, R. Shaw, and R. Walsh, *Chem. Rev.*, **69**, 279 (1969). o) "Selected Values of Chemical Thermodynamic Properties," Circular 500, National Bureau of Standards, Washington, D. C. (1952). p) L. Radom, W. J. Hehre, and J. A. Pople, *J. Am. Chem. Soc.*, **93**, 289 (1971). q) J. W. S. Jamieson and C. A. Winkler, *J. Phys. Chem.*, **60**, 1542 (1956). r) R. A. Nelson and R. S. Jessup, *J. Res. Natl. Bur. Stand.*, **48**, 206 (1952). s) I. Tokue, M. Ikarashi, and Y. Ito, *Bull. Chem. Soc. Jpn.*, **55**, 1250 (1982). t) W. H. Johnson, E. J. Prosen, and I. Jaffé, *J. Res. Natl. Bur. Std., Sect. A* **65**, 71 (1961).

Since the formation of ethylamine has been established by the NMR, IR, and MS measurements, it is clear that the first excited singlet $NH(a^1\Delta)$ formed by the photolysis of HN_3 at 313 nm[1] reacts to give ethylamine by the insertion into a C–H bond of C_2H_6. The formation of ethylamine has also been found in the photolysis of HN_3 in liquid ethane.[8] Reaction 4 is a collisional spin relaxation process of $NH(a^1\Delta)$ by C_2H_6 as was found for Xe.[1] Similar collisional quenching processes have also been found for the other excited singlet species.[10]

Since the $C_2H_5NH_2$* formed by Reaction 3 possesses excess energy in excess of 470 kJ mol^{-1}, Reactions 5 and 6 are energetically possible. The unimolecular decomposition of $C_2H_5NH_2$* to give $C_2H_4+NH_3$, $C_2H_2+NH_3+H_2$, and $CH_4+HCN+H_2$ is possible, but these reactions are excluded, because C_2H_4, C_2H_2, and HCN were not detected in the products. The decompositions of $C_2H_5NH_2$* to give $H_2+C_2H_5N$, $C_2H_5+NH_2$, $H+C_2H_6N$, and CH_4+CH_2=NH are also possible energetically. However, the possibilities of these reactions could not be established in the reaction kinetics, although the kinetics for the formations of H_2, CH_4, and NH_4N_3 were treated with scrupulous care as mentioned later.

On the other hand, Lovas *et al.*[11] have reported that ethylamine decomposes thermally to give $NH_3+C_2H_4$, CH_2=NH+CH_4, CH_2=$CHNH_2+H_2$, and CH_3CH=NH+H_2 at about 900 °C. The difference in reaction mechanism seems to be due to the reaction conditions, that is, the thermal decomposition at high temperatures and the unimolecular decomposition of the chemically activated $C_2H_5NH_2$* at room temperature.

Reaction 7 is a collisional deactivation process of the vibrationally excited $C_2H_5NH_2$* by a third body(M). Similar collisional deactivation processes have also been found in the $O(^1D)$[2] and $CH_2(^1A_1)$[4] systems.

The CH_2NH_2 radicals formed by Reaction 5 disappear to give CH_3NH_2 and N_3 by a hydrogen abstraction reaction from HN_3, and to give CH_3N_3 and NH_2 *via* addition to a π bond of HN_3 in Reactions 8 and 9. Both reactions are supported by the formations of CH_3NH_2 and CH_3N_3. Reaction 18 is a hydrogen abstraction reaction by CH_3 from HN_3 as a strong hydrogen donor. Konar *et al.*[12] have obtained $k_{18}=8.9\times10^7$ cm^3 mol^{-1} s^{-1} in the photolysis of azomethane in the presence of HN_3 at 25 °C.

Reaction 22 was proved by the experimental fact[9] that basic ammonia and amines of CH_3NH_2 and C_2H_5-NH_2, (RNH_2), react with acidic HN_3 in the vapor phase to give the azide salts ($RNH_2\cdot HN_3$) as a white volatile powder.

In the presence of HN_3, the reactions of $NH(X^3\Sigma^-)+C_2H_6\rightarrow NH_2+C_2H_5$ and $H+C_2H_6\rightarrow H_2+C_2H_5$ could not be found in the reaction kinetics for the formations of H_2 and NH_4N_3. Reactions other than those mentioned above were discussed previously,[1] and are omitted here.

At high light intensities, the formation of HCN is observed. Moreover, as seen in Fig. 4, $\phi_{NH_4N_3}$ increases, but ϕ_{N_2}, ϕ_{CH_4}, and $\phi_{CH_3NH_2}$ decrease with an increase of the light intensity. It is clear that these facts are due to some radical-radical reactions at high light intesities. The most abundant radical in this system will be $A\cdot N_3$, because the other radicals disappear and are converted into N_3 radicals by reactions with HN_3 as Reactions 8, 11, 12, 18, and 19. The N_3 radicals then rapidly become $A\cdot N_3$, most probably by addition as Reaction

20, with HN_3.[13] Thus, the following reactions

$$CH_3 + A\cdot N_3 \longrightarrow CH_3N_3 + A, \quad (23)$$

$$CH_2NH_2 + A\cdot N_3 \longrightarrow (N_3CH_2NH_2) + A, \quad (24)$$

were added at high light intensities. By the inclusion of the above reactions, we can explain not only the formation of HCN, but also the trends shown in Fig. 4. These are also useful to ascertain the existences of CH_3, CH_2NH_2, and $A\cdot N_3(N_3)$ radicals.

Reaction Kinetics. The following reaction kinetics were formulated to confirm the mechanism of Reactions 1 to 22 and to obtain the rate constant ratios at low light intensities.

As to the formations of CH_4, $CH_3NH_2\cdot HN_3$, and $C_2H_5NH_2\cdot HN_3$, the equation

$$\frac{\phi_{(CO_2)}}{\phi_{CH_4}} = \frac{k_8}{k_8+k_9} + \frac{2k_7(HN_3)[HN_3]}{k_5} + \frac{2k_7(C_2H_6)[C_2H_6]}{k_5}, \quad (I)$$

can be derived, where $\phi_{(CO_2)}$ denotes the total formation rate of CO_2 formed by the combustions of amine salts.

$$\phi_{(CO_2)} = \phi_{CH_3NH_2\cdot HN_3} + 2\,\phi_{C_2H_5NH_2\cdot HN_3}$$

plots of $\phi_{(CH_2)}/\phi_{CO_4}$ measured as a function of C_2H_6 pressure at 4.1 and 6.7 kPa of HN_3 are shown in Fig. 8, and the values of $k_9/k_8=0.852$, $k_7(HN_3)/k_5=3.03\times10^4$ $cm^3\,mol^{-1}$, and $k_7(C_2H_6)/k_5=3.65\times10^4$ $cm^3\,mol^{-1}$ are obtained from the intercepts and the slopes. Accordingly, the quantum yield of $CH_3NH_2.HN_3$ is given by the equation, $\phi_{CH_3NH_2\cdot HN_3}=[k_8/(k_8+k_9)]\phi_{CH_4}=0.540\ \phi_{CH_4}$.

In order to obtain the collisional deactivation efficiencies of $C_2H_5NH_2$* by Xe and CO_2, the photolysis of HN_3 in the presence of C_2H_6 and Xe or CO_2 was also carried out by the same method as mentioned above. Plots of $\phi_{(CO_2)}/\phi_{CH_4}$ measured as a function of Xe or CO_2 pressure at 6.7 kPa of HN_3 and 21.6 kPa of C_2H_6 are also shown in Fig. 8. The values of $k_7(Xe)/k_5=1.45\times10^4$ and $k_7(CO_2)/k_5=2.90\times10^4$ $cm^3\,mol^{-1}$ were obtained from the relation

$$\frac{\phi_{(CO_2)}}{\phi_{CH_4}} = \left(\frac{k_8}{k_8+k_9} + \frac{2k_7(HN_3)[HN_3]+2k_7(C_2H_6)[C_2H_6]}{k_5} + \frac{2k_7(Xe)[Xe]+2k_7(CO_2)[CO_2]}{k_5}\right), \quad (II)$$

and the slopes in Fig. 8.

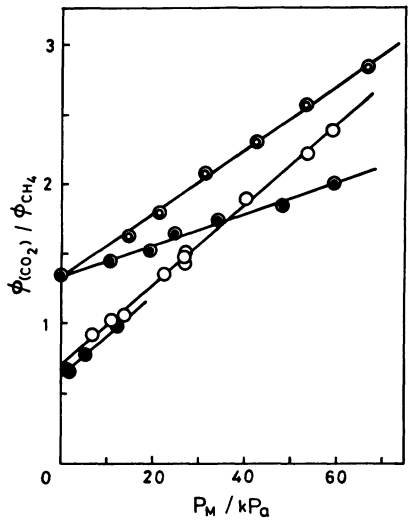

Fig. 8. Pressure dependence of $\phi_{(CO_2)}/\phi_{CH_4}$ at 313 nm and 30 °C. ◎, Measured as a function of CO_2 pressure at 6.7 kPa of HN_3 and 21.6 kPa of C_2H_6; ⊙, measured as a function of Xe pressure at 6.7 kPa of HN_3 and 21.6 kPa of C_2H_6; ○, measured as a function of C_2H_6 pressure at 6.7 kPa of HN_3; ●, measured as a function of C_2H_6 pressure at 4.1 kPa of HN_3.

On the formations of H_2, CH_4, NH_4N_3, $CH_3NH_2\cdot HN_3$, and $C_2H_5NH_2\cdot HN_3$, the equation

$$\left(\frac{\phi_{(N/4)}+\phi_{H_2}}{\phi_{CH_4}} - \frac{k_6}{k_5}\right)\frac{1}{\alpha} = 1 + \frac{k_4}{k_3} + \frac{k_2+k_{2a}}{k_3}\frac{[HN_3]}{[C_2H_6]}, \quad (III)$$

can be derived, where

$$\alpha = 1 + \frac{k_6}{k_5} + \frac{k_7(HN_3)[HN_3]+k_7(C_2H_6)[C_2H_6]}{k_5},$$

and

$$k_2 = k_{2a} + k_{2b} + k_{2c},$$

and $(N/4)$ means one-quater of total nitrogen atoms found in the combustions of azide salts.

$$\phi_{(N/4)} = \phi_{NH_4N_3} + \phi_{CH_3NH_2\cdot HN_3} + \phi_{C_2H_5NH_2\cdot HN_3}$$

Equation IV can be derived as to the formations of N_2, H_2, and CH_4.

$$\left(\frac{\phi_{N_2}+\phi_{H_2}}{\phi_{CH_4}} - \frac{3k_5+2k_6}{k_5}\right)\frac{1}{\alpha} = 1 + \frac{4k_4}{k_3} + 4\left(\frac{k_2+k_{2a}}{k_3}\right)\frac{[HN_3]}{[C_2H_6]} \quad (IV)$$

By combining Eqs. III and IV, the equation

$$\frac{4\phi_{(N/4)}+3\phi_{H_2}-\phi_{N_2}}{\phi_{CH_4}} - 3\left(\frac{k_7(HN_3)[HN_3]+k_7(C_2H_6)[C_2H_6]}{k_5}\right) = \frac{5k_6}{k_5}, \quad (V)$$

can be derived. By using the experimental values of $\phi_{(N/4)}$, ϕ_{N_2}, ϕ_{H_2}, and ϕ_{CH_4}, and the values of $k_7(HN_3)/k_5$ and $k_7(C_2H_6)/k_5$ obtained above, $k_6/k_5=0.038$ was obtained as a mean value.

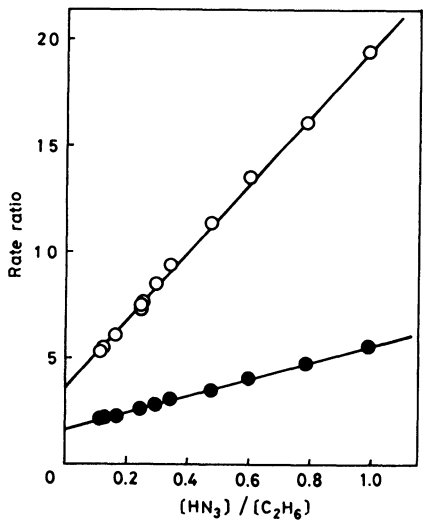

Fig. 9. Plots for Eqs. III and IV. ○, $[(\phi_{N_2}+\phi_{H_2})/\phi_{CH_4} - (3+2k_6/k_5)]/\alpha$; ●, $[(\phi_{(N/4)}+\phi_{H_2})/\phi_{CH_4} - k_6/k_5]/\alpha$. $k_6/k_5=0.038$.

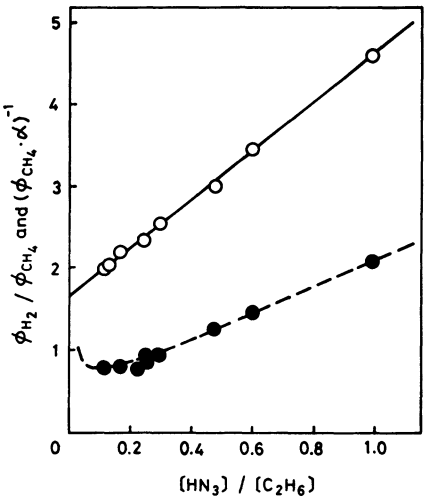

Fig. 10. Plots of $(\phi_{CH_4}\cdot\alpha)^{-1}$ and ϕ_{H_2}/ϕ_{CH_4} *versus* $[HN_3]/[C_2H_6]$. ○, $(\phi_{CH_4}\alpha)^{-1}$; ●, experimental value of ϕ_{H_2}/ϕ_{CH_4} at 6.7 kPa of HN_3; ---, calculated value of ϕ_{H_2}/ϕ_{CH_4} by Eq. VII.

The values of $[(\phi_{N_2}+\phi_{H_2})/\phi_{CH_4}-(3+2k_6/k_5)]/\alpha$ in Eq. IV were calculated using the experimental values and the rate constant ratios obtained above, and were plotted against $[HN_3]/[C_2H_6]$ as shown in Fig. 9. From the intercept and the slope, and from $k_{2b}/k_{2a}=0.746$ and $k_{2c}/k_{2a}=1.23$ obtained previously,[1] $k_3/k_2=0.334$ and $k_4/k_2=0.217$ were obtained. The relation of $[(\phi_{(N/4)}+\phi_{H_2})/\phi_{CH_4}-k_6/k_5]/\alpha$ *versus* $[HN_3]/[C_2H_6]$ in Eq. III was also plotted in Fig. 9, and the values of k_3/k_2 and k_4/k_2 obtained from the intercept and the slope were identical as those obtained from the plot for Eq. IV.

The values of k_3/k_2 and k_4/k_2 can also be obtained from the relation

$$\frac{1}{\phi_{CH_4}\alpha}=1+\frac{k_4}{k_3}+\frac{k_2}{k_3}\frac{[HN_3]}{[C_2H_6]}. \qquad \text{(VI)}$$

The values of k_3/k_2 and k_4/k_2 obtained from the straight line relation in Fig. 10 are consistent with those obtained from Eqs. III and IV.

To confirm the mechanism of succeeding reactions, the equation

$$\frac{\phi_{H_2}}{\phi_{CH_4}}=\frac{2k_6}{k_5}+\frac{k_4}{k_3}\frac{k_{10}\alpha}{k_{10}+k_{11}}+\frac{k_{2a}\alpha}{k_3}\left(\frac{2k_{12}}{k_{12}+k_{13}}+\frac{k_{2c}}{k_{2a}}\frac{k_{15}[HN_3]}{k_{14}+(k_{15}+k_{16})[HN_3]}\right)\frac{[HN_3]}{[C_2H_6]}, \qquad \text{(VII)}$$

was derived as to the formations of H_2 and CH_4. A plot of ϕ_{H_2}/ϕ_{CH_4} *versus* $[HN_3]/[C_2H_6]$ is shown in Fig. 10. The experimental values for ϕ_{H_2}/ϕ_{CH_4} are in good accord with the values calculated using the values of k_3/k_2, k_4/k_2, k_6/k_5, k_7/k_5, k_{2b}/k_{2a}, and k_{2c}/k_{2a} mentioned above, and of $k_{11}/k_{10}=3.22$, $k_{13}/k_{12}=1.15$, $k_{14}/k_{15}=2.27\times10^{-7}$ mol cm^{-3}, and $k_{16}/k_{15}=1.19$ obtained previously.[1] This means that the reaction mechanism and the rate constant ratios proposed previously[1] are also useful in the present system.

At high light intensities, the equation

$$\frac{\phi^*_{(CO_2)}-\beta\phi^\circ_{CH_4}}{\phi^*_{CH_4}}=\frac{k_8}{k_{18}}\frac{k_{23}}{k_{24}}+\left(1-\frac{k_8+k_9}{k_{18}}\frac{k_{23}}{k_{24}}\right)\left(\frac{\phi^*_{(CO_2)}}{\phi^\circ_{CH_4}}-\beta\right) \qquad \text{(VIII)}$$

can be derived for the formations of CH_4 and CO_2 by combustion, where

$$\beta=2(k_7(HN_3)[HN_3]+k_7(C_2H_6)[C_2H_6])/k_5$$

$\phi^*_{CH_4}$ and $\phi^*_{(CO_2)}$ denote the quantum yields of CH_4 and CO_2 at high light intensities. $\phi^\circ_{CH_4}$ is the estimated quantum yield of CH_4 at low light intensity, but the other experimental conditions are the same as those for $\phi^*_{CH_4}$ and $\phi^\circ_{CH_4}$. A plot of $(\phi^*_{(CO_2)}-\beta\phi^\circ_{CH_4})/\phi^*_{CH_4}$ *versus* $\phi^*_{(CO_2)}/\phi^\circ_{CH_4}-\beta$ is shown in Fig. 11. The values of $k_8k_{23}/k_{18}k_{24}=0.030$ from the intercept and $(k_8+k_9)k_{23}/k_{18}k_{24}=0.056$ from the slope were obtained. If we assumed that k_{23} is nearly equal to k_{24} because both reactions are the radical-radical combination,[14] $k_{18}/k_8=33.3$ and $k_{18}/(k_8+k_9)=18.0$ are obtained. These values imply that the reactivity of CH_2NH_2 for reaction with HN_3 is much lower than that of CH_3. It may be because CH_2NH_2 is stabilized by the interaction of an unpaired electron in CH_2 group with nonbonding electrons in NH_2 group.[15]

Comparisons of Rate Constants. The rate constant ratios for the reactions of $NH(a^1\Delta)$ are shown in Table 2, together with the values obtained by Tsunashima *et al.*[8] on the photolysis of HN_3 in liquid ethane at the Dry Ice–methanol temperature and 250 to 330 nm. The value of $k_3/(k_3+k_4)$ obtained by them is slightly higher than the value in the present work. The discrepancy may be due to the difference of the experimental conditions of phase, temperature, wavelength, *etc.*

On the other hand, their value for k_2/k_3 is extremely high as compared with our value. The most significant differences between the mechanisms are as follows: Reactions 2a, 2c, 10, and 13 were not taken into account in their mechanism; the reaction, $2NH_2\rightarrow N_2H_4$, was considered in their mechanism, although they failed to detect hydrazine.

The slope for Eq. III in Fig. 9 is steeper than the slope for Eq. VI in Fig. 10. This implies that k_{2a} is not zero.

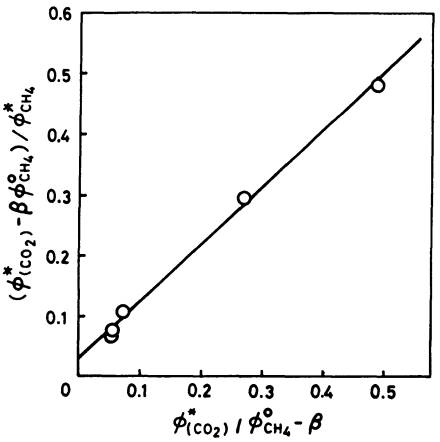

Fig. 11. Plot of $(\phi^*_{(CO_2)}-\beta\phi^\circ_{CH_4})/\phi^*_{CH_4}$ *versus* $\phi^*_{(CO_2)}/\phi^\circ_{CH_4}-\beta$.

TABLE 2. RATE CONSTANT RATIOS FOR THE REACTIONS OF $NH(a^1\Delta)$

$k_3/(k_3+k_4)$	k_2/k_3	
0.86 ± 0.04	125 ± 21	Ref. 8
0.606	2.99	This work

Moreover, if k_{2a} and k_{10} are zero, ϕ_{H_2}/ϕ_{CH_4} in Eq. VII should be reduced to 0.076 independently of $[HN_3]/[C_2H_6]$. This assumption is inconsistent with the experimental results of ϕ_{H_2}/ϕ_{CH_4} in Fig. 10. However, the large discrepancy for k_2/k_3 can not be explained by the existence of Reactions 2a, 10, and others, because the influence to k_2/k_3 on the succeeding reactions is not very large.

It seems that the reaction rate of NH($a^1\Delta$) with C_2H_6 is not very slow, judging from the specific rates of reactions of the first excited singlet species, C(2^1D_2),[16] O(2^1D_2),[17] and S(3^1D_2),[18] with CH_4, C_2H_6, C_3H_8, and others. The main reason for the large discrepancy of k_2/k_3 seems to be due to the difference of the liquid and vapor phases.

If we assume that the arrangement of molecules in the liquid is closest-packed hexagonal, and both C_2H_6 and HN_3 molecules have the same size and a spherical shape, HN_3 molecules are mutually separated by five molecular distances at the concentration ratio of $[HN_3]/[C_2H_6]=0.0034$. When a HN_3 molecule was converted into NH($a^1\Delta$) and N_2 by the photochemical decomposition, all of 322 molecules in four molecular layers from the central NH($a^1\Delta$) are ethane. Although twelve molecules of HN_3 exist at the fifth layer, the NH($a^1\Delta$) will be lost by an insertion or quenching reaction with C_2H_6 before the NH($a^1\Delta$) encounters a HN_3 molecule, because the set-collision with C_2H_6 as a solvent molecule takes place during the diffusion process.

Since the five molecule separation was merely taken as an average value, and the mutual diffusion between NH($a^1\Delta$) and HN_3 occurs during the reaction period, the situation is not quite so simple. However, the probability that the excited singlet NH($a^1\Delta$) encounters a HN_3 molecule will be much less than that expected from the concentration. This prediction drastically reduces the appearent k_2/k_3 value. Therefore, the high value for k_2/k_3 may be due to a contribution from succeeding reactions for NH($X^3\Sigma^-$).

The high value of k_2/k_3 is also explainable if dimers and clusters of HN_3 are formed in liquid ethane at Dry Ice–methanol temperature. However, it is uncertain at present if dimers and clusters are in fact formed hydrogen bonding and molecular association.

The specific rate of Reaction 7 can be estimated from the equation

$$k_7 = \eta\, k_z, \qquad \text{(IX)}$$

where, k_z is the collision number of $C_2H_5NH_2$* per second, and η is the collisional stabilization efficiency. The value of k_z can be calculated from the Lennard-Jones collision frequency.[19]

$$k_z = N_A\sigma^2_{B-M}(8\pi kT/\mu_{B-M})^{1/2}\Omega^{(2,2)*}_{B-M} \qquad \text{(X)}$$

Here, N_A is Av σ_{B-M} ogadro's number,and k is Boltzmann's constant. σ_{B-M}, μ_{B-M}, and $\Omega^{(2,2)*}_{B-M}$ mean the collision diameter, the reduced mass, and the reduced collision integral for B(ethylamine) and M molecules, respectively. The values of $\Omega^{(2,2)*}_{B-M}$ are conveniently tabulated[20] as a function of kT/ε_{B-M} with the Lennard-Jones well depth $\varepsilon_{B-M}=(\varepsilon_{B-B}\cdot\varepsilon_{M-M})^{1/2}$. The σ_{B-M} is given by $\sigma_{M-B}=(\sigma_B+\sigma_M)/2$. For ethylamine, $\sigma_B=4.80$ Å and $\varepsilon_{B-B}/k=320$ K were estimated from those for C_2H_5OH,[21] C_3H_6,[22] and C_3H_8[23] molecules. The values of k_z calculated using Eq. X are shown in Table 3.

The absolute value of k_5 can be estimated from the relation

$$k_5 = \eta k_z/(k_7/k_5)_{obsd}. \qquad \text{(XI)}$$

The values of k_5 calculated by assuming $\eta=1$ are shown in Table 3, and it is found that the values for C_2H_6, HN_3, and CO_2 are almost the same. This result means that the $C_2H_5NH_2$* is deactivated with every collision in the collisions with polyatomic molecules such as C_2H_6, HN_3, and CO_2.

The value of k_5 calculated with $\eta=1$ for Xe is higher than the values for the polyatomic molecules. Therefore the collisional deactivation efficiency of Xe is less than unity, and should be reduced to 0.60 to adjust to the same value as k_5 for polyatomic molecules. The result is supported by the fact that the collisional energy transfer efficiencies by monatomic molecules are much less than those by polyatomic molecules.[24]

As a specific rate of the unimolecular decomposition of $C_2H_5NH_2$* to give CH_3 and CH_2NH_2, $k_5=9.8\times10^9$ s^{-1} is obtained by averaging the three values for polyatomic molecules. From the rate constant ratio of $k_6/k_5=0.038$, $k_6=3.7\times10^8$ s^{-1} is obtained for the unimolecular decomposition of $C_2H_5NH_2$* to give CH_3-CN and $2H_2$. By using the relation $\tau=\ln 2/(k_5+k_6)$, $\tau=6.8\times10^{-11}$ s is obtained as a half life of $C_2H_5NH_2$*.

The author is gratefully indebted to Emeritus Professor Osamu Toyama of University of Osaka Prefecture for his helpful advice and to Dr. Sotaro Esho for his cooperation.

References

1) S. Kodama, *Bull. Chem. Soc. Jpn.*, **56**, 2348 (1983).
2) H. Yamazaki and R. J. Cvetanović, *J. Chem. Phys.*, **41**, 3703 (1964); W. B. DeMore and O. F. Raper, *ibid.*, **46**, 2500

Table 3. Calculated values of k_5 and k_7 at 30 °C

M	σ_M Å	ε_{M-M}/k K	k_Z 10^{14} cm^3 mol^{-1} s^{-1}	$(k_7/k_5)_{obsd}$ 10^4 cm^3 mol^{-1}	$k_5(\eta=1)$ 10^9 s^{-1}	k_7 10^{14} cm^3 mol^{-1} s^{-1}
C_2H_6	4.42[a]	230[a]	3.60	3.65	9.86	3.60
HN_3	3.96[b]	240[b]	2.98	3.03	9.83	2.98
CO_2	3.75[c]	246[c]	2.83	2.90	9.76	2.83
Xe	3.97[d]	228[d]	2.39	1.45	16.48	1.42

a) J. Roberts, *Brit. Chem. Eng.*, **8**, 753 (1963). b) Estimated values. c) A. A. Clifford, P. Gray, and N. Platts, *J. Chem. Soc., Faraday Trans. 1*, **73**, 381 (1977). d) E. A. Mason and W. E. Rice, *J. Chem. Phys.*, **22**, 843 (1954).

(1967); L. M. Quick and R. J. Cvetanović, *Can. J. Chem.*, **49**, 2193 (1971); A. J. Colussi and R. J. Cvetanović, *J. Phys. Chem.*, **79**, 1891 (1975).

3) H. E. Gunning and O. P. Strausz, *Adv. Photochem.*, **4**, 143 (1966).

4) P. M. Crane and T. L. Rose, *J. Phys. Chem.*, **79**, 403 (1975); K. Shibuya, K. Obi, and I. Tanaka, *Bull. Chem. Soc. Jpn.*, **49**, 2178 (1976); H. M. Frey and G. J. Kennedy, *J. Chem. Soc., Faraday Trans. 1*, **73**, 164 (1977); A. D. Clements, H. M. Frey, and R. Walsh, *ibid.*, **73**, 1340 (1977).

5) E. D. Miller, Ph. D. Dissertation, Catholic University of America, Washington, D. C., 1961.

6) D. W. Cornell, R. S. Berry, and W. Lwoski, *J. Am. Chem. Soc.*, **88**, 544 (1966).

7) J. L. Brash and R. A. Back, *Can. J. Chem.*, **43**, 1778 (1965).

8) S. Tsunashima, J. Hamada, M. Hotta, and S. Sato, *Bull. Chem. Soc. Jpn.*, **53**, 2443 (1980).

9) These samples were prepared by the following methods: an amine was mixed with small excess of HN_3 in the vapor phase, and the salt formed was purified by evacuating excess HN_3 at the Dry Ice–acetone temperature.

10) J. A. Bell, *J. Phys. Chem.*, **75**, 1537 (1971); D. J. Little, A. Dalgleish, and R. J. Donovan, *Discuss. Faraday Soc.*, **53**, 211 (1972); S. T. Amimoto, A. P. Force, R. G. Gulotty, and J. R. Wiesenfeld, *J. Chem. Phys.*, **71**, 3640 (1979); D. Husain and D. P. Newton, *J. Chem. Soc., Faraday Trans. 2*, **78**, 51 (1982).

11) F. J. Lovas, F. O. Clark, and E. Tiemann, *J. Chem. Phys.*, **62**, 1925 (1975).

12) R. S. Konar and B. DEB. Darwent, *Can. J. Chem.*, **48**, 2280 (1970).

13) R. J. Paur and E. J. Bair, *J. Photochem.*, **1**, 255 (1973); R. J. Paur and E. J. Bair, *Int. J. Chem. Kinet.*, **8**, 139 (1976).

14) T. S. Lee, T. Ree, H. Eyring, and T. Fueno, *J. Chem. Phys.*, **36**, 281 (1962); M. J. Gibian and R. C. Corley, *Chem. Rev.*, **73**, 441 (1973).

15) C. A. Coulson and J. Jacobs, *J. Chem. Soc.*, **1949**, 1983; H. H. Jaffé, *J. Chem. Phys.*, **20**, 279 (1952); A. Pullman, *Bull. Soc. Chim. Fr.*, **1958**, 641.

16) D. Husain and L. J. Kirsch, *Trans. Faraday Soc.*, **67**, 2886, 3166 (1971).

17) P. Michaud, G. Paraskevopoulos, R. J. Cvetanović, *J. Phys. Chem.*, **78**, 1457 (1974); I. S. Fletcher and D. Husain, *Can. J. Chem.*, **54**, 1765 (1976); J. A. Davidson, H. I. Schiff, G. E. Stereit, J. R. McAfee, A. L. Schmeltekopf, and C. J. Howard, *J. Chem. Phys.*, **67**, 5021 (1977).

18) R. J. Donovan and D. Husain, *Chem. Rev.*, **70**, 489 (1970).

19) J. Troe, *J. Phys. Chem.*, **83**, 114 (1979).

20) J. O. Hirschfelder, R. B. Bird, and E. L. Spotz, *J. Chem. Phys.*, **16**, 968 (1948); J. O. Hirschfelder, C. F. Curtiss, and R. B. Bird, "Molecular Theory of Gases and Liquids," Wiley (1954), p. 1126.

21) L. Monchick and E. A. Mason, *J. Chem. Phys.*, **35**, 1676 (1961).

22) Ed. by S. Gratch, "Advances in Thermophysical Properties at Extreame Temperatures and Pressures," ASME (1965).

23) L. S. Tee, S. Gotoh, and W. E. Stwart, *Ind. Eng. Chem., Fundam.*, **5**, 356 (1966).

24) P. J. Marcoux, E. E. Siefert, and D. W. Setser, *Int. J. Chem. Kinet.*, **7**, 473 (1975); P. J. Marcoux and D. W. Setser, *J. Phys. Chem.*, **82**, 97 (1978).